

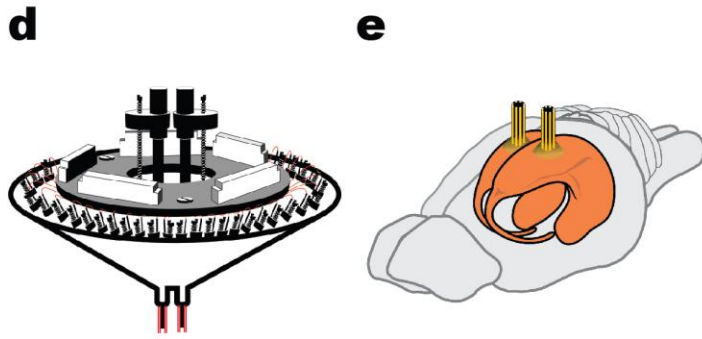
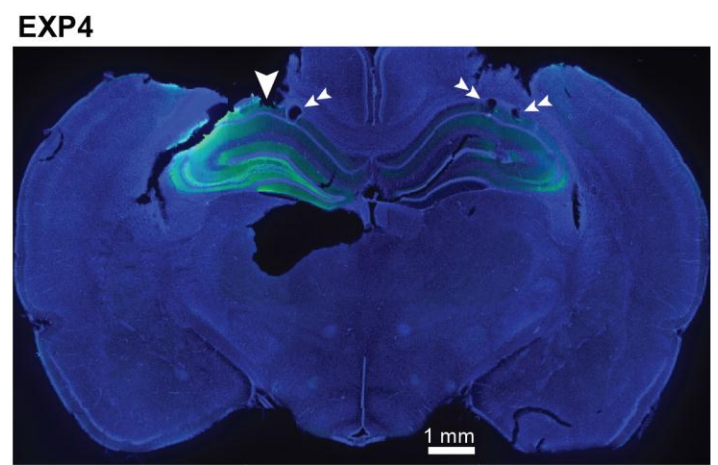
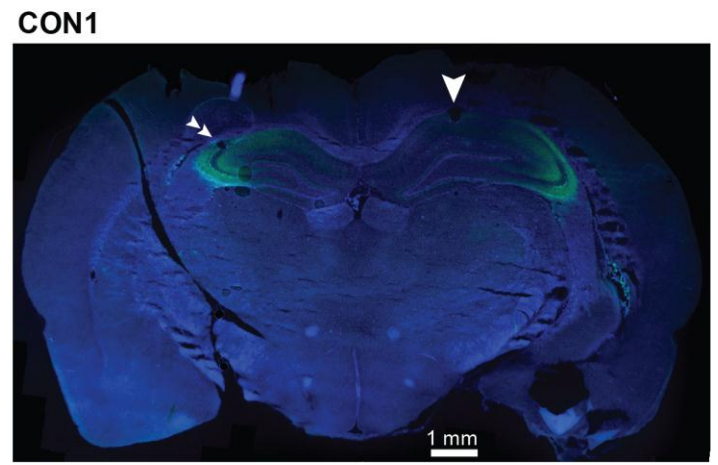
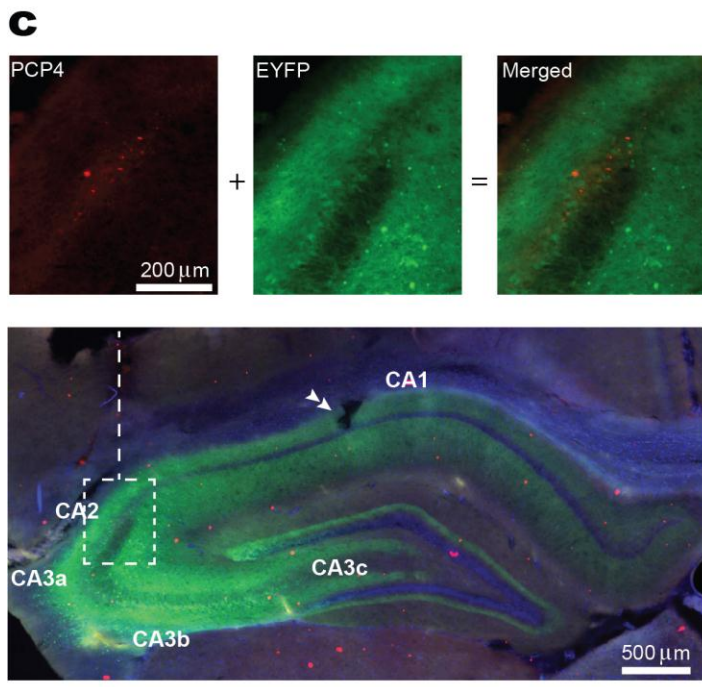
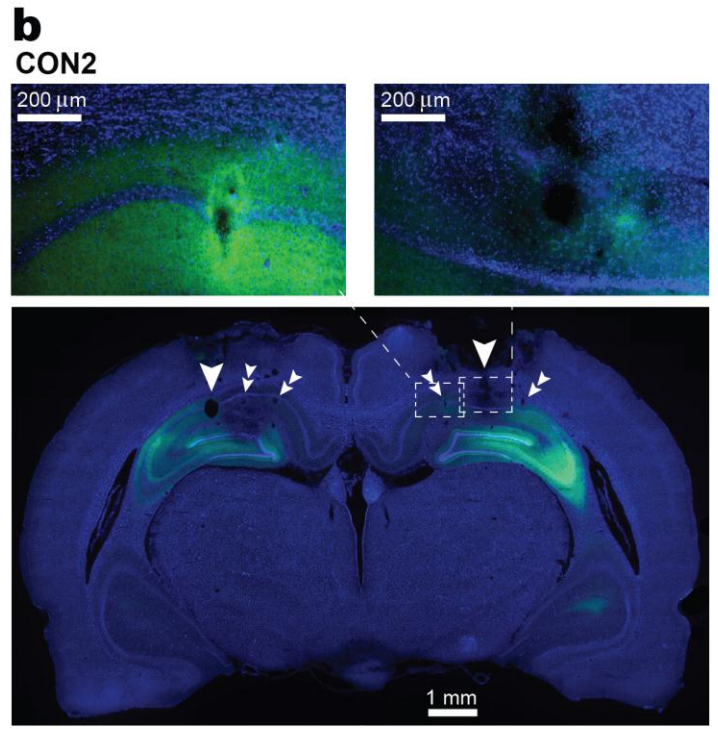
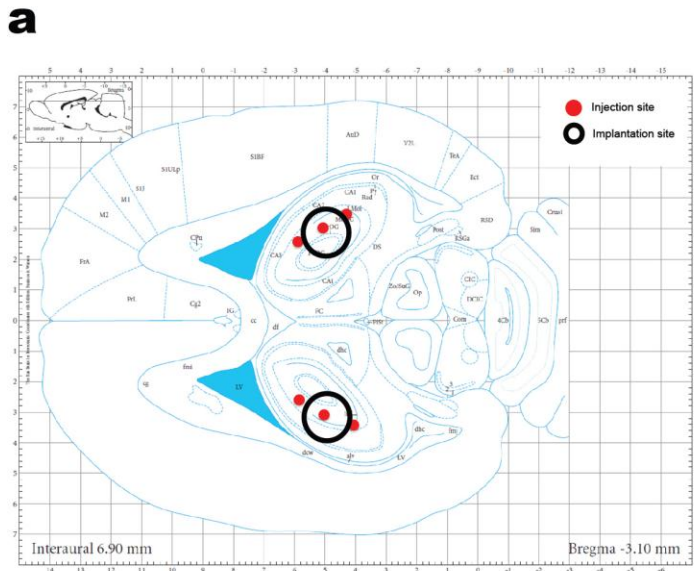


In the format provided by the authors and unedited.

Acute silencing of hippocampal CA3 reveals a dominant role in place field responses

Heydar Davoudi ^{1,2,3,4} and David J. Foster ^{1,2,3*}

¹Department of Psychology, University of California, Berkeley, Berkeley, CA, USA. ²Helen Wills Neuroscience Institute, University of California, Berkeley, Berkeley, CA, USA. ³Solomon H. Snyder Department of Neuroscience, Johns Hopkins University School of Medicine, Baltimore, MD, USA. ⁴Department of Biomedical Engineering, Johns Hopkins University School of Medicine, Baltimore, MD, USA. *e-mail: davidfoster@berkeley.edu



SupplementaryFigure 1

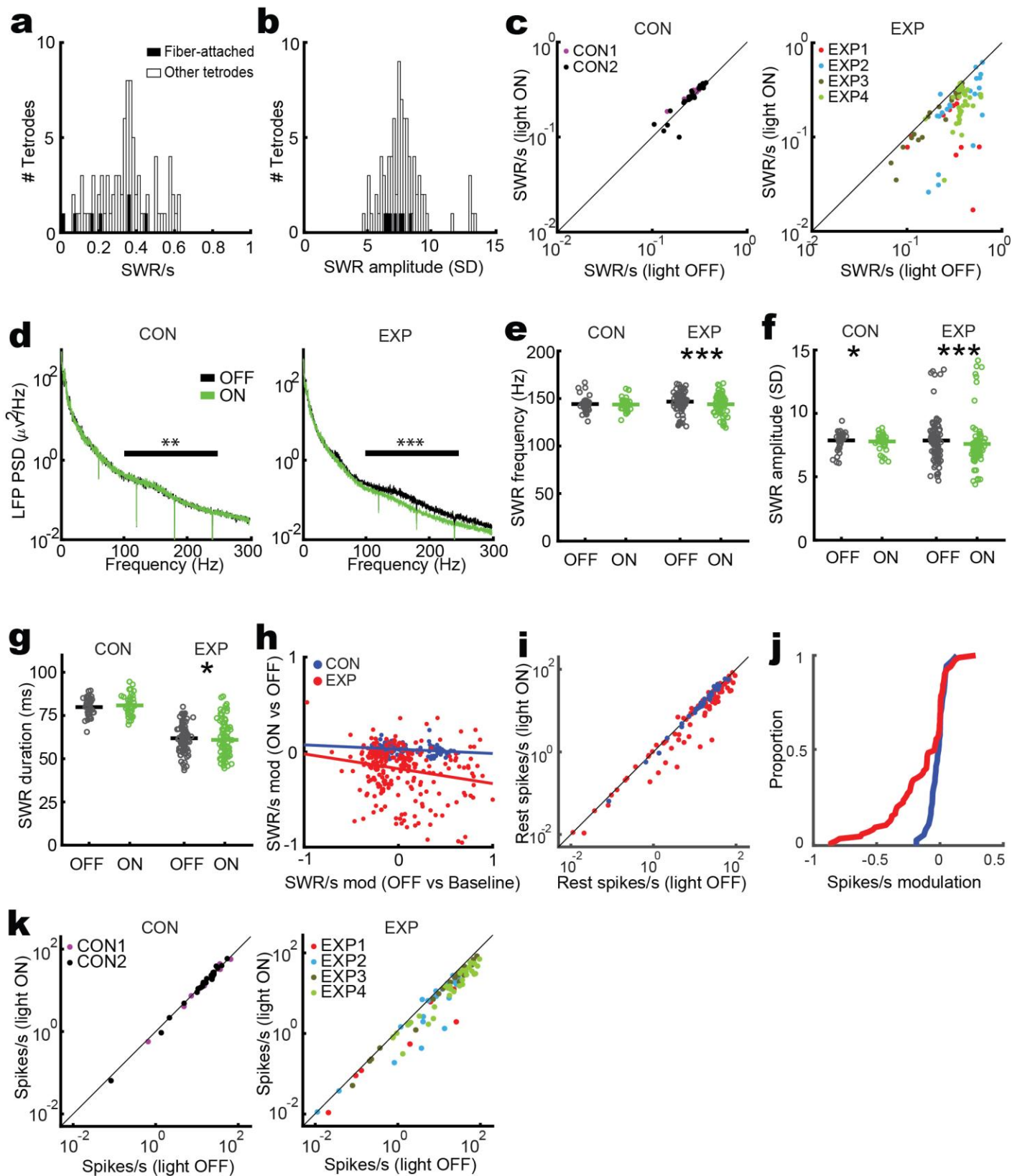
Viral expression, optetrode design, and optical fiber and tetrode locations

a) Six injection sites in dorsal and intermediate CA3 are shown in red are overlaid on a rat brain atlas. Black circles display the location of optetrode implanted in second surgery.

b) Histology of three preserved rat brains used in this study show repeatable anatomical and expression results. GFP expression (green) is overlaid on background Hoechst 33258 signal (blue). Optical fiber and tetrode locations are shown with large arrowheads and small double-arrowheads, respectively. Top Zoomed-in figures demonstrate an optical fiber location (right) with an adjacent tetrode (left). CA3 projects to both stratum radiatum and stratum oriens in CA1 (green signal, top left). Note that tetrodes that are away from the fiber still can be modulated by laser light. This is because light can open eArch3.0 proton pumps in the middle of axons and inhibit the transmission of action potentials to axon end terminals.

c) An example hippocampal slice showing GFP expression is limited to CA3 and does not protrude CA2. The three-color immunohistochemistry with Hoechst 33258 (blue), CA2 marker PCP4 (red), and EYFP (green) depicts that the viral injection and consequent GFP expression was in CA3b and CA3a subregions and barely reached to CA2. Top insets show the expressions in the dashed rectangle. Also note that CA3a-b project comparably to both strata radiatum and oriens in CA1. A tetrode location is demonstrated with a small double-arrowhead. The large red dots in the lower panel are due to a non-perfect rinsing of secondary antibody during immunohistochemistry. Since our brain tissues were old we had a technical problem in acquiring a high quality immunohistochemistry for PCP4 protein in individual rats. Therefore, we only present one rat with an acceptable PCP4 labeling and instead emphasize more on the other two sources of evidence (i.e. anatomical (**b**) and electrophysiological (**Supplementary Figure 2a-b**) to verify the specificity of our inactivation.

d-e) The designed optetrode with 40 tetrodes. Both fibers and tetrodes are individually and independently adjustable.



Supplementary Figure 2

CA3 input is necessary for resting-state activity in CA1 in sleep box.

a-b) SWR activity in fiber-attached tetrodes is not significantly different from other tetrodes and this implies that they are located in the same CA1 layer. **a)** SWR incidence rate in light OFF condition in EXP rats in sleep box (fiber-attached vs others: 0.23 ± 0.06 (mean \pm s.e.m) for all values in this figure legend) SWR/s vs 0.35 ± 0.015 , $n_1 = 7$ and $n_2 = 85$ tetrodes, two-tailed rank sum test, $Z_{(91)} = -1.6$, $p = 0.12$). **b)** SWR amplitude in light OFF condition in EXP rats in sleep box (fiber-attached vs others: 7.22 ± 0.27 SD vs 7.86 ± 0.20 , $n_1 = 7$ and $n_2 = 85$ tetrodes, two-tailed rank sum test, $Z_{(91)} = -1.0$, $p = 0.3$). There were 8 fiber-attached tetrodes (one per hemisphere) for four EXP rats and one of them was broken (therefore: $n_1 = 7$).

c) Effect of light on rest-state CA1 SWR activity in individual rats. SWR incidence rate for each tetrode in light ON vs. light OFF conditions colored for individual CON (left) and EXP (right) rats. The suppression effect was significant in all four individual EXP rats.

d) Power spectral density (PSD) of raw LFP during light OFF (black) and light ON (green) conditions. The LFP power in the ripple frequency range (100- 250 Hz) is marked by horizontal black bars. EXP tetrodes show a significant decrease in ripple band power of their raw LFPs, reaffirming the suppression of SWR activity during rest state (CON: OFF: $24.37 \pm 1.81 \mu V^2$ and ON: 24.93 ± 1.84 , two-tailed paired t-test after logarithmic transformation, $n = 37$ tetrodes, $F_{(36)} = 9.0$, $p = 0.005$; EXP: OFF: 17.38 ± 2.65 and ON: 11.79 ± 1.41 , two-tailed paired t-test after logarithmic transformation, $n = 88$ tetrodes, $F_{(87)} = 56.8$, $p = 5 \times 10^{-11}$).

e-g) Effect of light on SWR characteristics in sleep box. SWR peak power frequency (**e**), amplitude (**f**), and duration (**g**) calculated from SWRs occurring in OFF and ON conditions. **e)** SWR power peak frequency was slightly decreased in EXP rats during ON periods (CON: OFF: 144.10 ± 1.33 Hz and ON: 143.68 ± 1.15 , two-tailed signed rank test, $n = 37$ tetrodes, $Z_{(36)} = 1.0$, $p = 0.3$; EXP: OFF: 147.05 ± 1.02 and ON: 144.25 ± 1.03 , two-tailed signed rank test, $n = 88$ tetrodes, $Z_{(87)} = 4.8$, $p = 2 \times 10^{-6}$). **f)** SWR amplitude was slightly decreased in EXP rats during light ON periods (CON: OFF: 7.86 ± 0.13 SD and ON: 7.78 ± 0.11 , two-tailed signed rank test, $n = 37$ tetrodes, $Z_{(36)} = 2.0$, $p = 0.046$; EXP: OFF: 7.85 ± 0.19 and ON: 7.56 ± 0.20 , two-tailed signed rank test, $n = 88$ tetrodes, $Z_{(87)} = 3.7$, $p = 3 \times 10^{-4}$). **g)** SWR duration remained intact in both EXP and CON tetrodes (CON: OFF: 79.81 ± 0.88 ms and ON: 80.84 ± 1.04 , two-tailed paired t-test, $n = 37$ tetrodes, $F_{(36)} = -4.0$, $p = 0.05$; EXP: OFF: 61.99 ± 0.85 and ON: 60.86 ± 1.11 , two-tailed signed rank test, $n = 88$ tetrodes, $Z_{(87)} = 2.5$, $p = 0.02$).

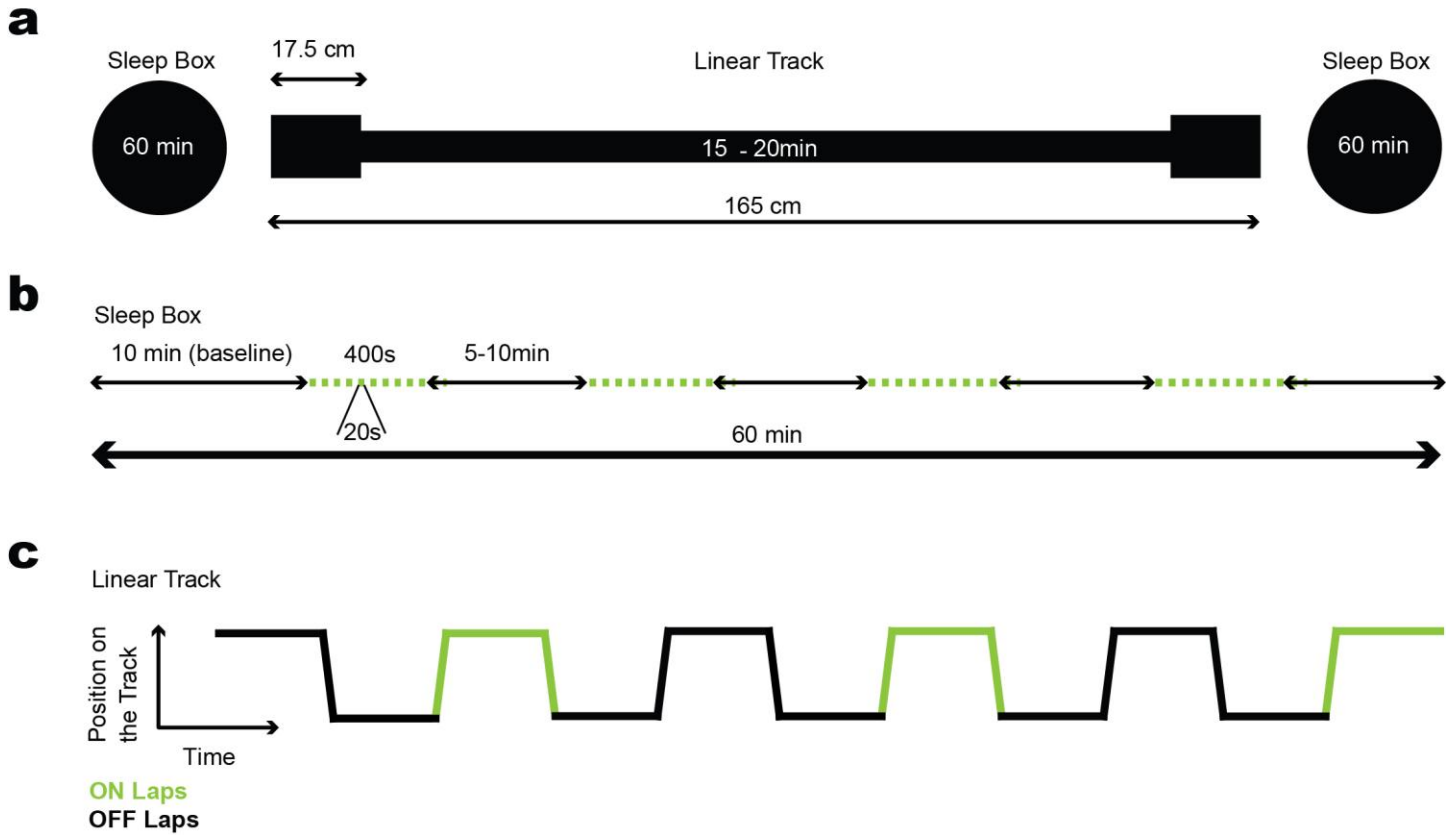
h) Subtle rebound effect is observed in light-suppressed EXP tetrodes. SWR incidence rate was not significantly different in light OFF vs. baseline conditions in both CON and EXP tetrodes (CON: baseline: 0.23 ± 0.01 SWR/s and OFF: 0.27 ± 0.01 , two-tailed signed rank test, $n = 108$ tetrodes, $Z_{(107)} = -1.2$, $p = 0.22$; EXP: baseline: 0.32 ± 0.01 and OFF: 0.31 ± 0.01 , two-tailed signed rank test, $n = 253$ tetrodes, $Z_{(252)} = 0.4$, $p = 0.7$). But, SWR incidence in light ON condition was lower than the baseline in EXP tetrodes (baseline: 0.32 ± 0.01 SWR/s and ON: 0.22 ± 0.01 , two-tailed signed rank test, $n = 253$ tetrodes, $Z_{(252)} = 7.2$, $p = 10^{-12}$). However, in EXP rats, SWR incidence rate modulation in light OFF vs Baseline (i.e. (OFF-Baseline)/(OFF+Baseline)) is negatively correlated with that of ON vs OFF (i.e. (ON-OFF)/(ON+OFF)) (Pearson's correlation: CON: $n = 108$ tetrodes, $r = -0.18$, $p = 0.057$; EXP: $n = 252$ tetrodes, $r = -0.21$, $p = 0.0008$). This implies that the greater the suppression of tetrodes by laser light, the greater the increase in SWR incidence rate (compared to baseline) when light becomes OFF. Each dot represents a CON (blue) or EXP (red) tetrode and only for this panel repetitive tetrodes from different recording sessions are included.

i) Rest multi-unit activity for each tetrode in light ON vs. light OFF conditions in CON (OFF: 19.59 ± 2.45 spikes/s and ON: 19.65 ± 2.49 , two-tailed signed rank test, $n = 36$ tetrodes, $Z_{(35)} = 0.3$, $p = 0.8$) and EXP (OFF: 24.41 ± 2.68 and ON: 18.95 ± 2.19 , two-tailed signed rank test, $n = 84$ tetrodes, $Z_{(83)} = 4.5$, $p = 10^{-5}$) rats. Each dot represents a tetrode and colors are as in **h**.

j) Cumulative density plot of the amount of modulation of spiking activity by light in CON (blue) and EXP (red) tetrodes (two-tailed rank sum test: $n_1 = 36$ and $n_2 = 84$ tetrodes, $Z_{(120)} = 4.0$, $p = 0.004$). Each dot represents a tetrode and blue and red colors represent CON and EXP rats, respectively.

k) Effect of light on rest-state CA1 spiking activity in individual rats. Multi-unit activity for each tetrode in light ON vs. light OFF conditions colored for individual CON (left) and EXP (right) rats. In all of these scatter plots, each dot represents a tetrode.

* $P < 0.05$, *** $P < 0.001$.



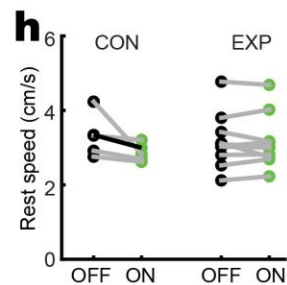
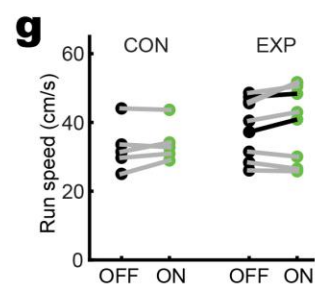
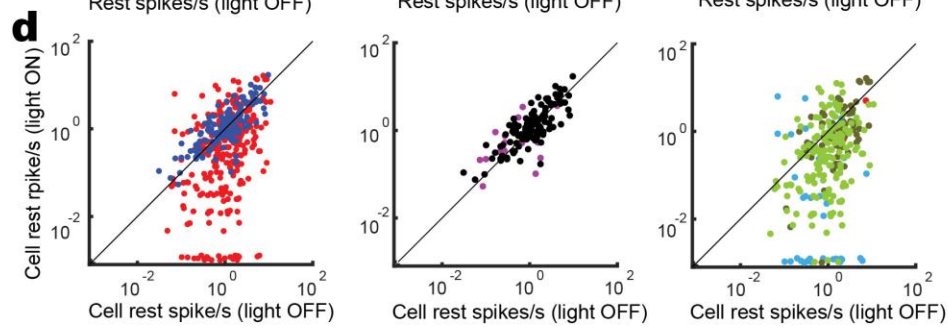
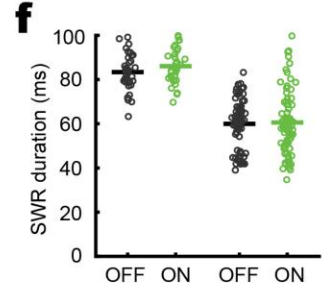
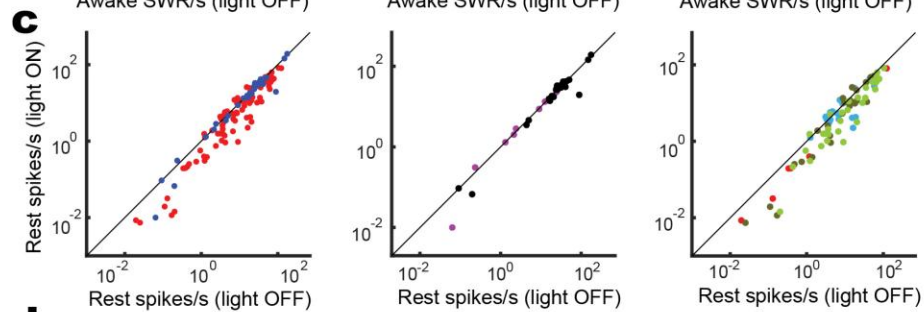
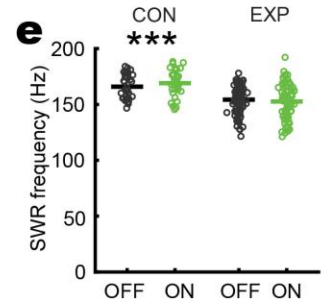
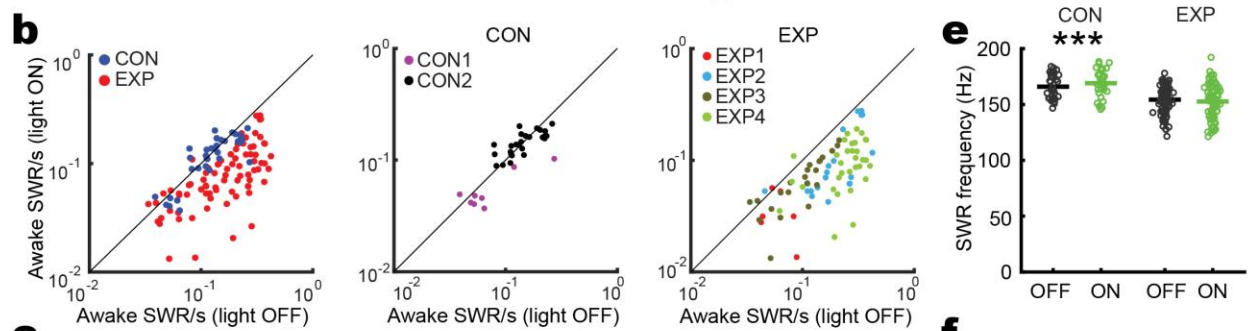
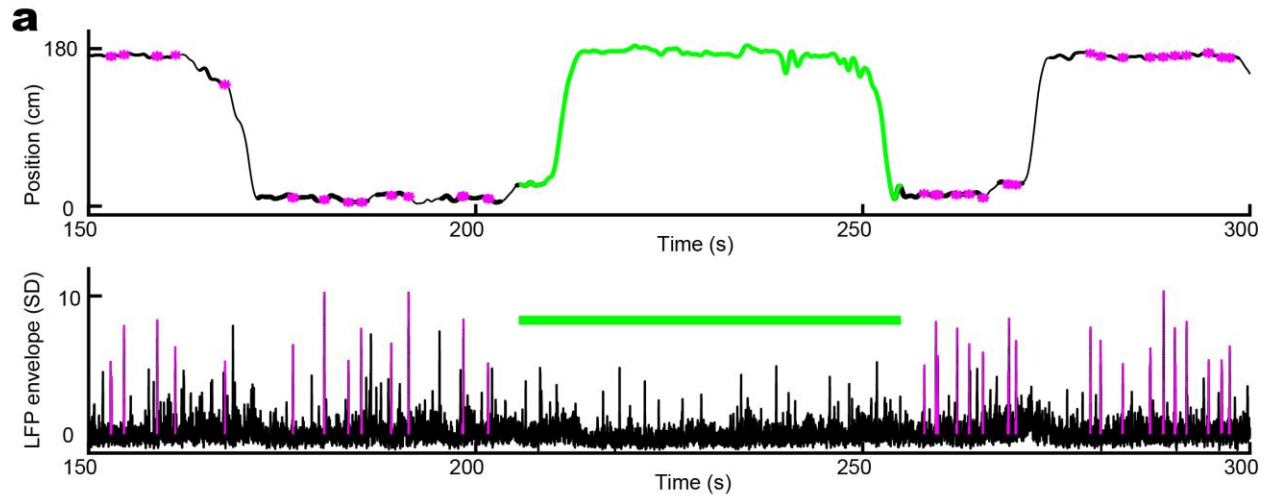
Supplementary Figure 3

The experimental design and laser stimulation framework.

a) Schematic of an experimental session containing recordings from a rat in a sleep box, followed by linear track traversals, and then returning to the same sleep box.

b) In the sleep box, optical silencing is performed by four pulse trains each lasting 400 seconds. Each train consists of ten 20-s-long stimulations separated by ten 20-s-long light off time spans.

c) For the track traversal session, light is manually and consecutively turned on and off for ON and OFF laps. ON laps consisted of forward run, a pause at one end of the track to consume fluid reward, and then a run to the other end of the track.



Supplementary Figure 4

CA3 input is necessary for resting-state activity in CA1 during exploratory behavior.

a) An example tetrode in CA1 region shows strong SWR modulation by silencing CA3 input to CA1 (above) when a rat stays at one end of track. Each magenta star marker (above) and line (below) depicts a detected SWR event. The thick black line shows the moments that the rat's speed was less than 7 cm/sec ("rest" time spans).

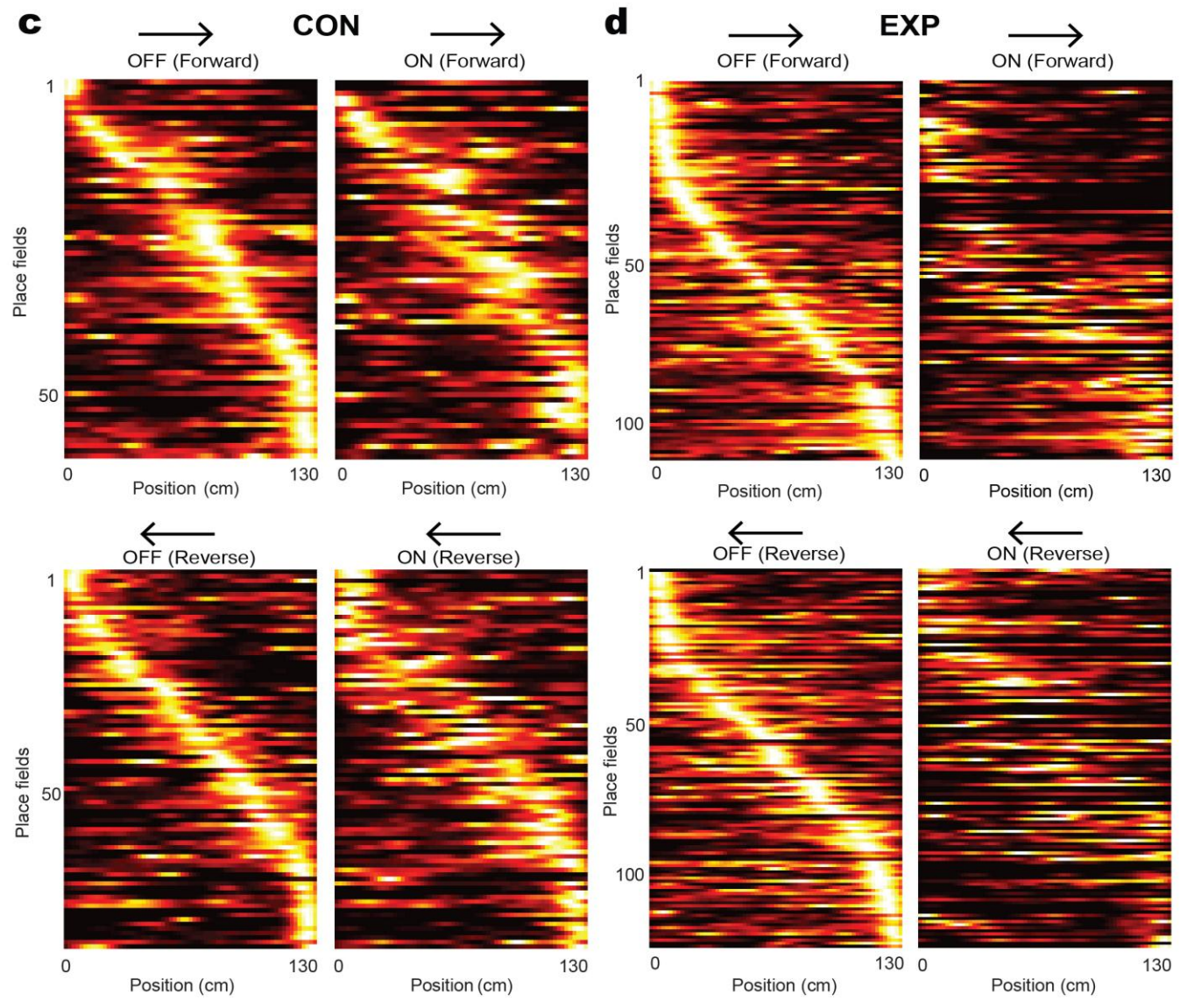
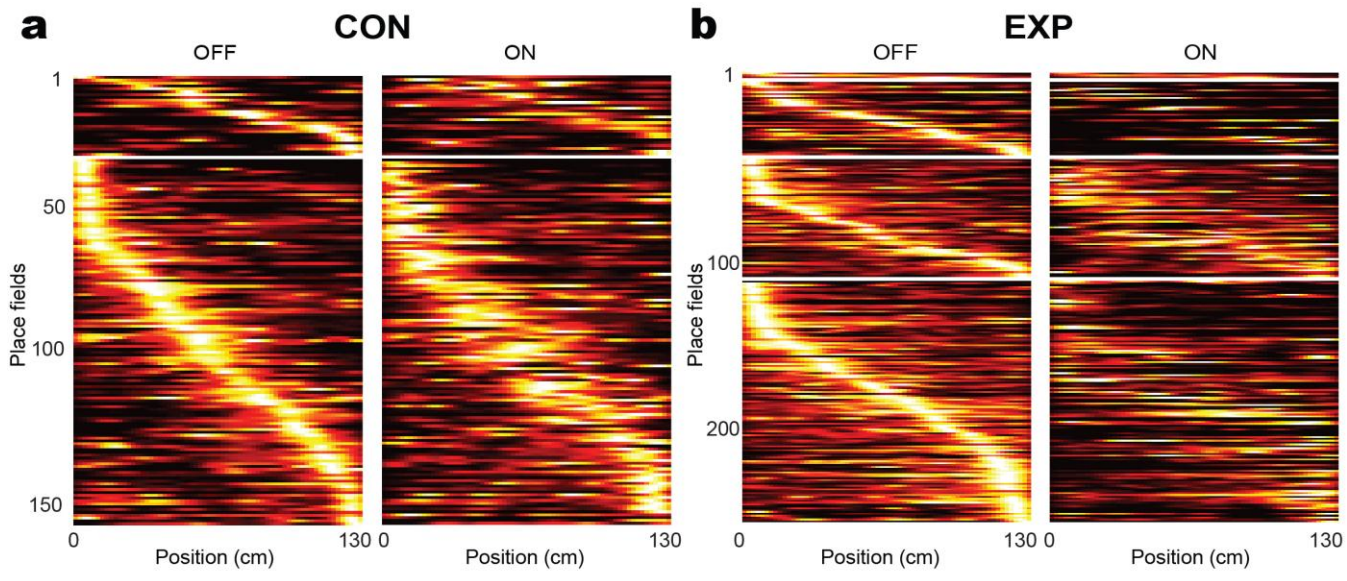
b) Incidence of SWR events for each tetrode in light ON vs. light OFF conditions only considering rest moments. The effect of silencing in individual rats is shown in the middle and lower panels for CON and EXP rats, respectively. silencing CA3 input to CA1 strongly suppressed the incidence rate of SWRs in EXP tetrodes, while slightly increasing the incidence rate in CON tetrodes (CON: OFF: 0.13 ± 0.01 (mean \pm s.e.m for all values in this figure legend) SWR/s and ON: 0.12 ± 0.01 , two-tailed paired t-test, $n = 34$ tetrodes, $F_{(33)} = 2.8$, $p = 0.10$; EXP: OFF: 0.18 ± 0.01 and ON: 0.08 ± 0.01 , two-tailed signed rank test, $n = 80$ tetrodes, $Z_{(79)} = 7.6$, $p = 3 \times 10^{-14}$). This suppression effect was significantly observed in all individual EXP rats.

c) multi-unit spiking activity gets suppressed in light ON condition in EXP tetrodes (CON: OFF: 29.76 ± 6.41 spikes/s and ON: 28.17 ± 6.45 , two-tailed signed rank test, $n = 35$ tetrodes, $Z_{(34)} = 0.6$, $p = 0.6$; EXP: OFF: 19.06 ± 2.87 , ON: 13.08 ± 2.05 , two-tailed signed rank test, $n = 81$ tetrodes, $Z_{(80)} = 5.2$, $p = 5 \times 10^{-7}$). This effect was significant for all individual EXP rats except one rat.

d) Single unit spiking activity for each putative pyramidal cell in CA1 show suppression in condition in EXP rats (CON: OFF: 1.71 ± 0.16 Hz and ON: 2.60 ± 0.25 , two-tailed signed rank test, $n = 132$ cells, $Z_{(131)} = -1.8$, $p = 0.066$, EXP: OFF: 1.71 ± 0.11 and ON: 1.36 ± 0.16 , two-tailed signed rank test, $n = 262$ cells, $Z_{(261)} = 5.7$, $p = 10^{-8}$). In **b** and **c**, each dot represents a tetrode while in **d** each dot represents a pyramidal cell. Blue and red colors represent EXP and CON rats, respectively. Tetrodes or cells that were completely silenced were assigned with a fixed low value only for visualization purpose in these logarithmic plots.

e-f) Subtle abnormalities in awake SWRs. Ripple peak power frequency (**e**) and duration (**f**) calculated from SWRs occurring in OFF and ON conditions in CON (left) and EXP (right) rats. **e)** SWR peak power frequency is slightly increased in CON tetrodes (CON: OFF: 166.45 ± 1.80 Hz and ON: 169.82 ± 1.95 , two-tailed paired t-test, $n = 34$ tetrodes, $F_{(33)} = 17.2$, $p = 0.0002$; EXP: OFF: 153.50 ± 1.46 and ON: 152.11 ± 1.68 , two-tailed paired t-test, $n = 80$ tetrodes, $F_{(79)} = 3.7$, $p = 0.059$). **f)** SWR duration did not shift in light ON condition in CON and EXP rats (CON: OFF: 83.13 ± 1.42 ms and ON: 85.90 ± 1.33 , two-tailed signed rank test, $n = 34$ tetrodes, $F_{(33)} = 3.2$, $p = 0.08$; EXP: OFF: 59.79 ± 1.22 and ON: 60.41 ± 1.62 , two-tailed signed rank test, $n = 80$ tetrodes, $Z_{(79)} = -0.6$, $p = 0.5$).

g-h) Laser light does not affect animal behavior. For each recording session, OFF (black marker) and ON (green marker) are depicted in relation to each other. **g)** run speed (CON: OFF: 32.78 ± 3.16 cm/s and ON: 34.10 ± 2.55 , two-tailed paired t-test, $n = 5$ sessions, $F_{(4)} = 2.2$, $p = 0.21$; EXP: OFF: 39.03 ± 2.89 and ON: 40.93 ± 3.60 , two-tailed paired t-test, $n = 9$ sessions, $F_{(8)} = 4.0$, $p = 0.8$). **h)** rest speed (CON: OFF: 3.31 ± 0.26 cm/s and ON: 2.87 ± 0.11 , two-tailed paired t-test, $n = 5$, $F_{(4)} = 3.4$, $p = 0.14$; EXP: 3.10 ± 0.24 and 3.06 ± 0.22 , two-tailed signed rank test, $n = 9$ sessions, $Z_{(8)} = 0.7$, $p = 0.7$). Pairs with significant lap-by-lap difference (two-tailed signed rank test, $p < 0.05$) are connected with dark lines and pairs with non-significant difference are shown with transparent lines. *** denotes $p < 0.001$.



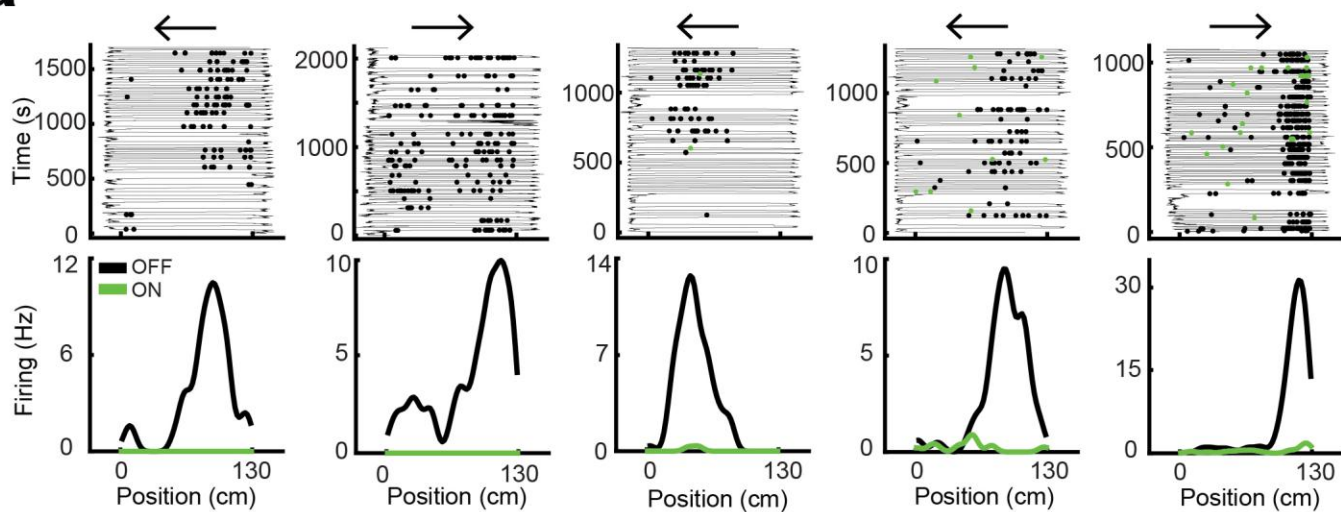
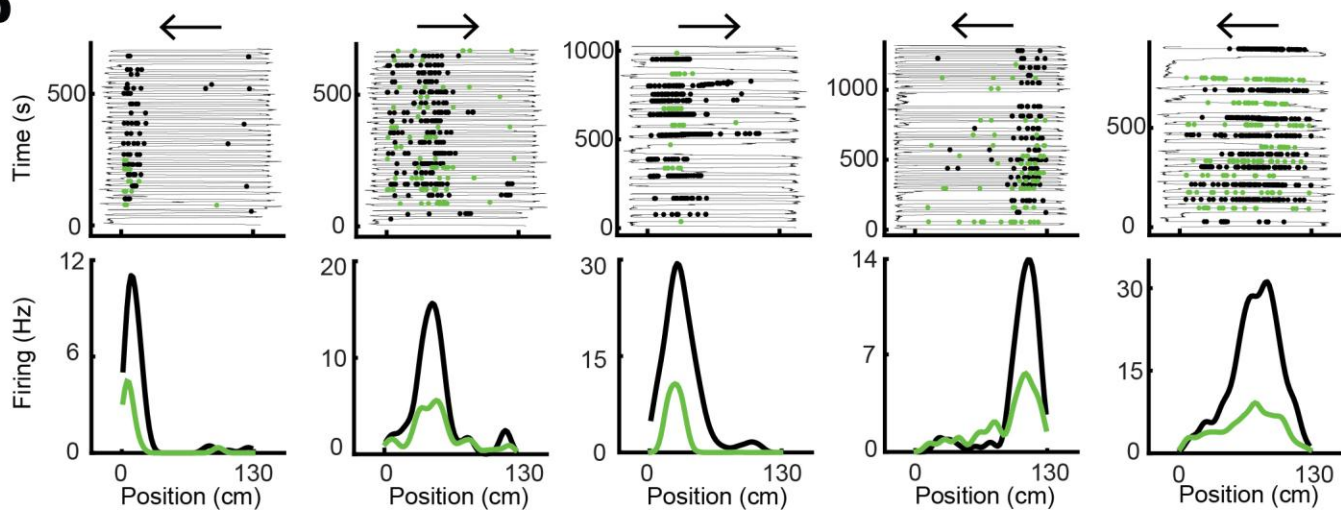
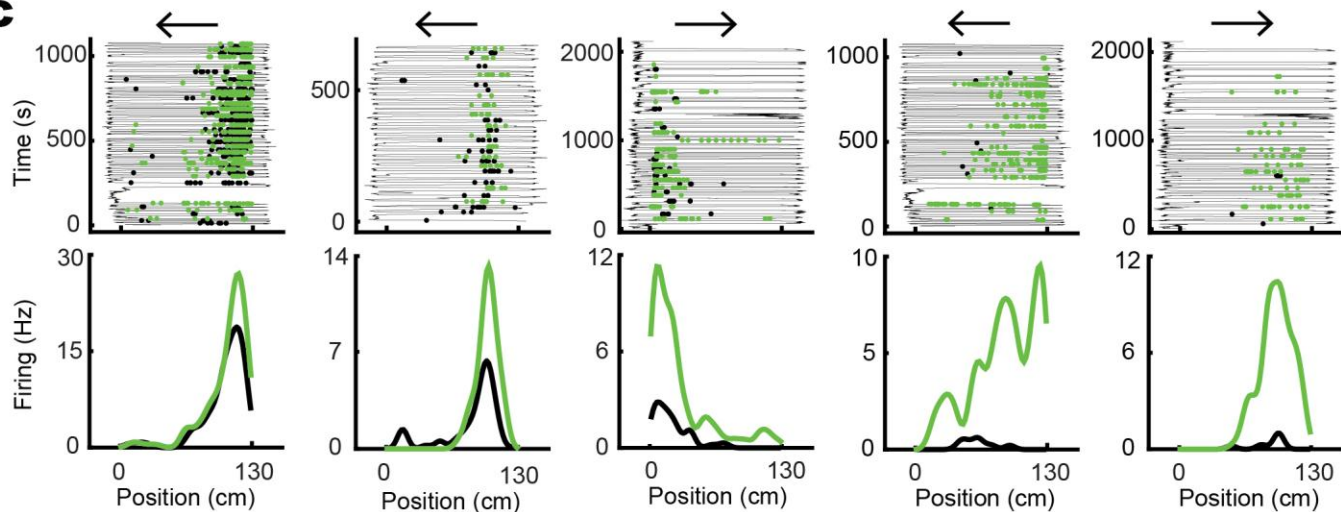
Supplementary Figure 5

Place-cell firing in CON and EXP rats.

a-b) All place fields for two CON (**a**) and three EXP rats (**b**) are sorted by their peak firing position on linear track during light OFF condition. Each row depicts color map of the same place field in light OFF (left) and ON (right) conditions. Both OFF and ON fields are normalized by maximum peak firing rate in either conditions.

c-d) CON and EXP Place fields sorted by running directions of rats on the track. "Forward" (rightward arrows) is the direction that laser alternatively starts to shine light and "reverse" (leftward arrows) is the returning direction of animal where at its end the laser turns off in every other lap. Each row depicts color map of the same place field in light OFF (left) and ON (right) conditions for CON (**c**) and EXP (**d**) rats.

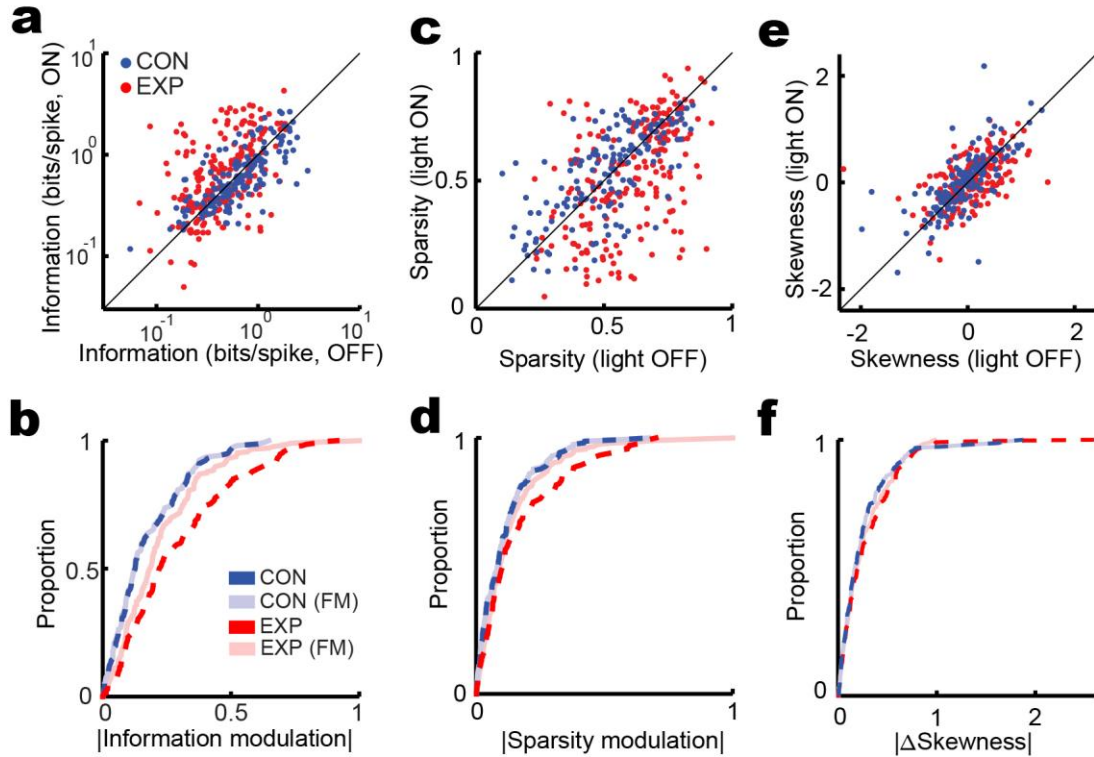
Results were independently repeatable for the two CON and the four EXP rats.

a**b****c**

Supplementary Figure 6

Examples of suppressed and enhanced EXP place fields

Examples of CA1 place fields for light OFF (black) and ON (green) conditions in EXP rats. Top: rat position is shown as a function of time during linear track traversals (thin line), overlaid with spiking activity of the above place cell (dots) only in the running direction depicted by the arrow. Spikes in OFF and ON conditions are shown as black and green dots, respectively. Bottom: The average place field calculated from above lap-by-lap spiking activity during light OFF (black) and light ON (green) conditions. Examples of complete or dramatic silencing (**a**), partial silencing (**b**), and partial enhancement to rarely-found place field emergence (**c**) are shown respectively. Results were independently repeatable for the two CON and the four EXP rats.



Supplementary Figure 7

Place-field features are degraded during suppression of CA3 input

a) Spatial information is significantly increased in EXP place fields in light ON condition (CON: OFF: 0.79 ± 0.04 (mean \pm s.e.m for all values in this figure legend) bits/spike and ON: 0.73 ± 0.04 , two-tailed paired t-test after logarithmic transformation, $n = 156$ fields, $F_{(155)} = 2.6$, $p = 0.11$; EXP: OFF: 0.55 ± 0.03 and ON: 0.86 ± 0.05 , two-tailed signed rank test, $n = 208$ fields, $Z_{(207)} = -6.3$, $p = 5 \times 10^{-10}$).

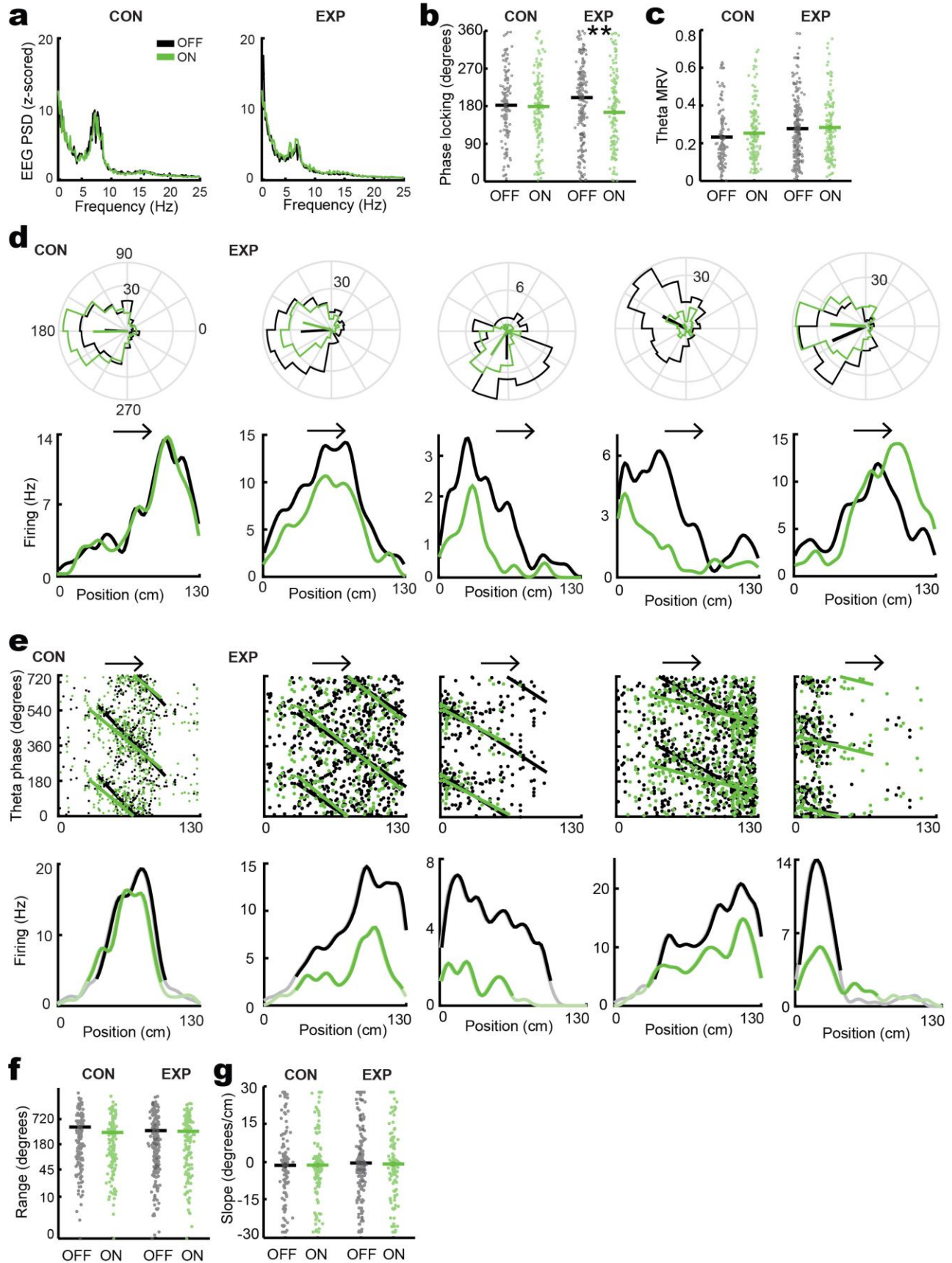
b) The cumulative density plot of the absolute value of the amount of spatial information modulation of original (**a**) and firing-matched (FM) place fields (Original: two-tailed rank sum test, $n_1 = 156$ and $n_2 = 208$ fields, $Z_{(362)} = -5.3$, $p = 10^{-7}$; FM: two-tailed rank sum test, $n_1 = 156$ and $n_2 = 207$ fields, $Z_{(362)} = -3.2$, $p = 0.0013$; EXP original vs EXP FM: $n = 208$ fields, $Z_{(362)} = 5.6$, $p = 3 \times 10^{-8}$).

c) Place field sparsity is suppressed in light ON condition in EXP rats. (CON: OFF: 0.52 ± 0.01 and ON: 0.53 ± 0.01 , two-tailed signed rank test, $n = 156$ fields, $Z_{(155)} = -1.5$, $p = 0.13$; EXP: OFF: 0.60 ± 0.01 and ON: 0.52 ± 0.02 , two-tailed signed rank test, $n = 207$ fields, $Z_{(206)} = 5.4$, $p = 10^{-7}$).

d) The CDF of the absolute value of the amount of sparsity modulation of original (**c**) and FM place fields (Original: two-tailed rank sum test, $n_1 = 156$ and $n_2 = 207$, $Z_{(362)} = 2.7$, $p = 0.007$; FM: two-tailed rank sum test, $n_1 = 156$ and $n_2 = 207$, $Z_{(362)} = 1.6$, $p = 0.11$).

e) Place field skewness does not show a directional shift in light ON condition in EXP rats. (CON: OFF: -0.07 ± 0.04 and ON: -0.01 ± 0.04 , two-tailed paired t-test, $n = 156$ fields, $F_{(155)} = 4.0$, $p = 0.047$; EXP: OFF: 0.03 ± 0.03 and ON: 0.15 ± 0.03 , two-tailed paired t-test, $n = 207$ fields, $F_{(206)} = 0.6$, $p = 0.5$).

f) The CDF of the absolute value of the amount of skewness shift of original (**e**) and firing-matched place fields shows no significant difference between CON and EXP rats. ($|\Delta$ Skewness|: Original: two-tailed rank sum test, $n_1 = 156$ and $n_2 = 207$ fields, $Z_{(362)} = 1.3$, $p = 0.21$; FM: two-tailed rank sum test, $n_1 = 156$ and $n_2 = 207$ fields, $Z_{(362)} = -3.3$, $p = 0.001$; EXP original vs EXP FM: two-tailed signed rank test, $n = 207$ fields, $Z_{(362)} = 0.6$, $p = 0.5$).



Supplementary Figure 8

Examples of place-cell theta locking

a) PSD of z-scored CA1 LFP during track traversals in light OFF (black) and light ON (green) conditions is not significantly affected in CON and EXP tetrodes in theta frequency band (5-10 Hz) (CON: two-tailed paired t-test, $n = 34$ tetrodes, $F_{(33)} = 0.8$, $p = 0.4$; EXP: two-tailed signed rank test, $n = 80$ tetrodes, $Z_{(79)} = -1.5$, $p = 0.14$).

b) Theta locking preference is shifted in EXP place fields in light ON condition (CON: OFF: $182.26 \pm 5.57^\circ$ (mean \pm s.e.m for all values in this figure legend), Rayleigh test for circular non-uniformity, $n = 135$ fields, $Z_{(134)} = 17.3$, $p = 2 \times 10^{-8}$ and ON: $179.14 \pm 5.52^\circ$, Rayleigh test, $n = 144$ fields, $Z_{(143)} = 15.8$, $p = 10^{-7}$, Watson-Williams test for circular comparison, $n_1 = 135$ and $n_2 = 144$ fields, $F_{(278)} = 0.1$, $p = 0.8$; EXP: OFF: $200.44 \pm 4.90^\circ$, Rayleigh test, $n = 217$ fields, $Z_{(216)} = 9.2$, $p = 10^{-4}$; ON: $165.23 \pm 5.95^\circ$, Rayleigh test, $n = 142$ fields, $Z_{(141)} = 7.8$, $p = 5 \times 10^{-4}$, Watson-Williams test, $n_1 = 217$ and $n_2 = 142$ fields, $F_{(358)} = 8.4$, $p = 0.004$).

c) Theta locking strength measured by MRV is not affected by light (CON: OFF: 0.23 ± 0.01 and ON: 0.25 ± 0.01 , two-tailed rank-sum test, $n_1 = 135$ and $n_2 = 144$ fields, $Z_{(278)} = -1.3$, $p = 0.19$; EXP: OFF: 0.28 ± 0.01 and ON: 0.28 ± 0.01 , two-tailed rank-sum test, $n_1 = 217$ and $n_2 = 142$ fields, $Z_{(358)} = -0.2$, $p = 0.9$). In **b-c** all place fields were considered for analysis though place fields with significant theta tuning also show similar results.

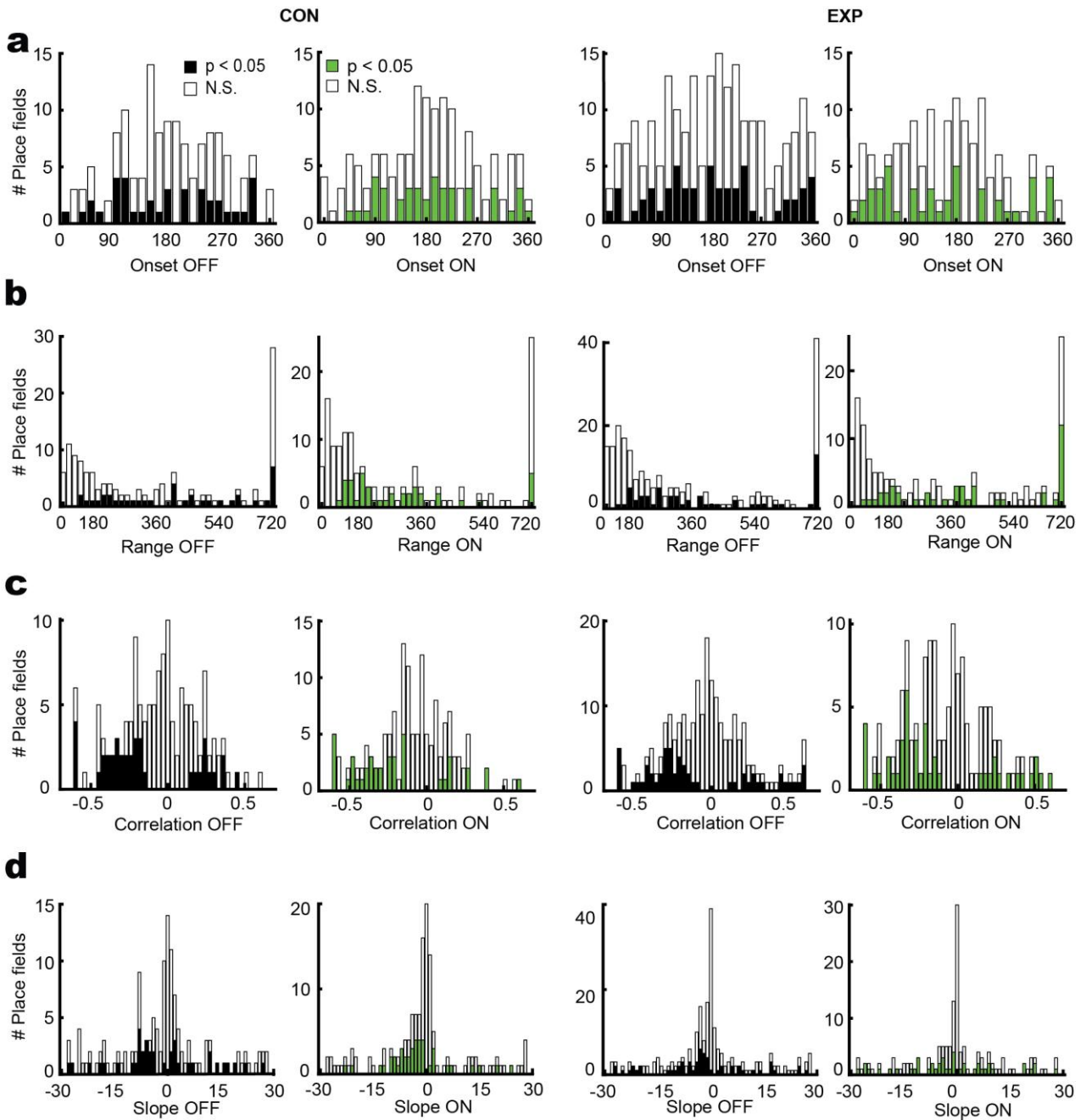
d) Examples of place field theta locking in CON and EXP rats. Top: Theta phase preference of individual place fields during light OFF (black) and light ON (green) conditions. The corresponding black and green bars in each polar plot indicate the mean resultant vector (MRV) for each condition. Bottom: The corresponding place field, calculated in the direction shown by the arrow, during light OFF (black) and ON (green) conditions. Results were independently repeatable for the two CON and the four EXP rats.

e) Four examples of place field theta phase precession in EXP rats. Top: Each dot represents the theta phase of individual spikes occurring either during light OFF (black) or light ON (green) conditions in relation to its position on the linear track. Bottom: Associated place fields in light OFF (black) and light ON (green) conditions. Results were independently repeatable for the two CON and the four EXP rats.

f) Phase precession range remains intact in light ON condition (CON: OFF: $465.78 \pm 48.68^\circ$ and ON: $346.74 \pm 36.43^\circ$, two-tailed rank-sum test, $n_1 = 135$ and $n_2 = 144$ fields, $Z_{(278)} = 1.7$, $p = 0.09$; EXP: OFF: $381.35 \pm 33.32^\circ$ and ON: $367.01 \pm 33.35^\circ$, two-tailed rank-sum test, $n_1 = 217$ and $n_2 = 142$ fields, $Z_{(358)} = -0.4$, $p = 0.7$).

g) Phase precession slope remains intact in light ON condition (CON: OFF: $-1.25 \pm 1.11^\circ/\text{cm}$ and ON: -1.17 ± 0.99 , two-tailed rank sum test, $n_1 = 135$ and $n_2 = 144$ fields, $Z_{(278)} = 0.1$, $p = 0.8$; EXP: OFF: -0.34 ± 0.82 and ON: -0.74 ± 1.02 , two-tailed rank-sum test, $n_1 = 217$ and $n_2 = 142$ fields, $Z_{(358)} = 0.2$, $p = 0.9$).

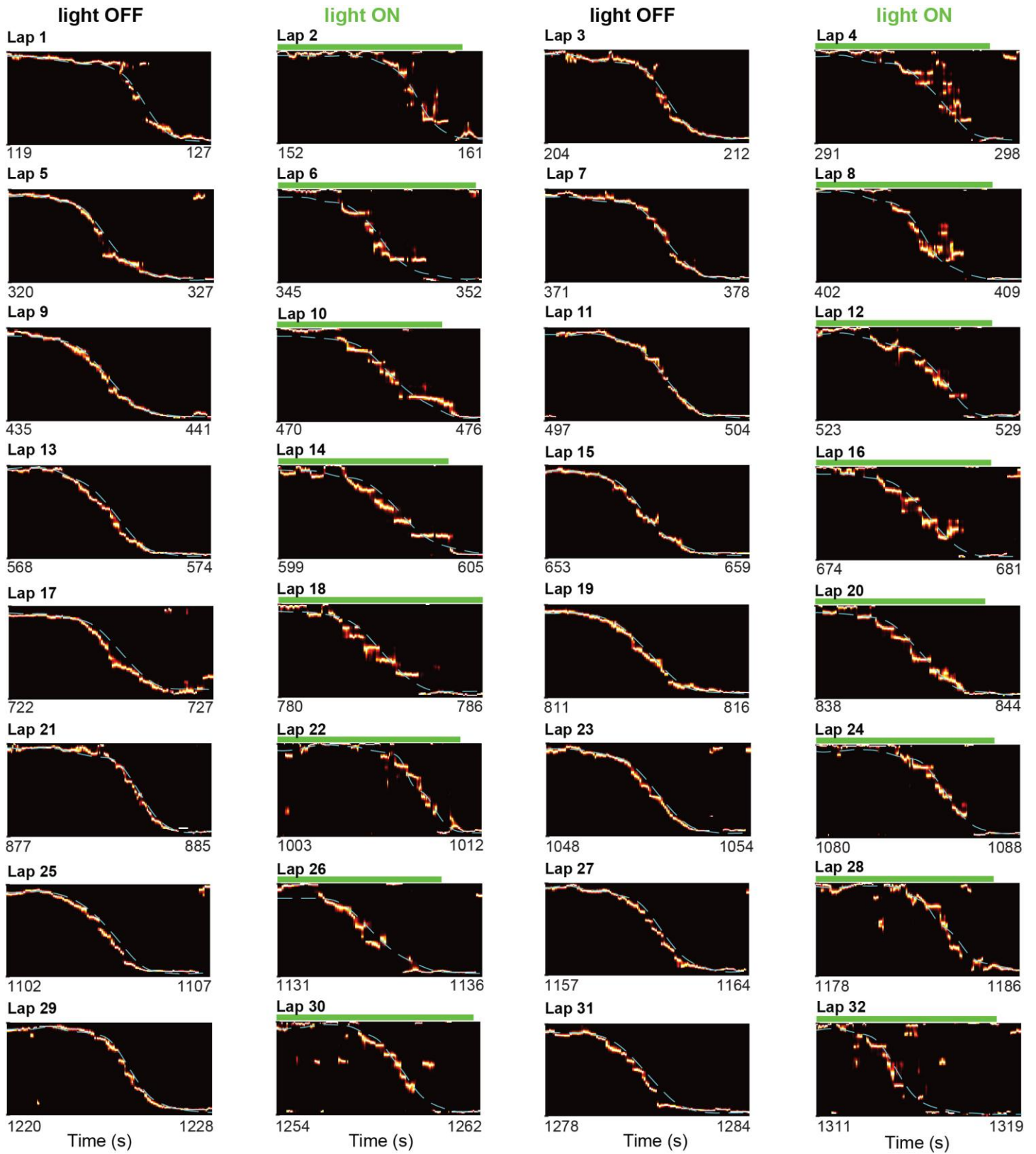
* $P < 0.05$, ** $P < 0.01$.



Supplementary Figure 9

Phase-precession characteristics in CON and EXP place fields

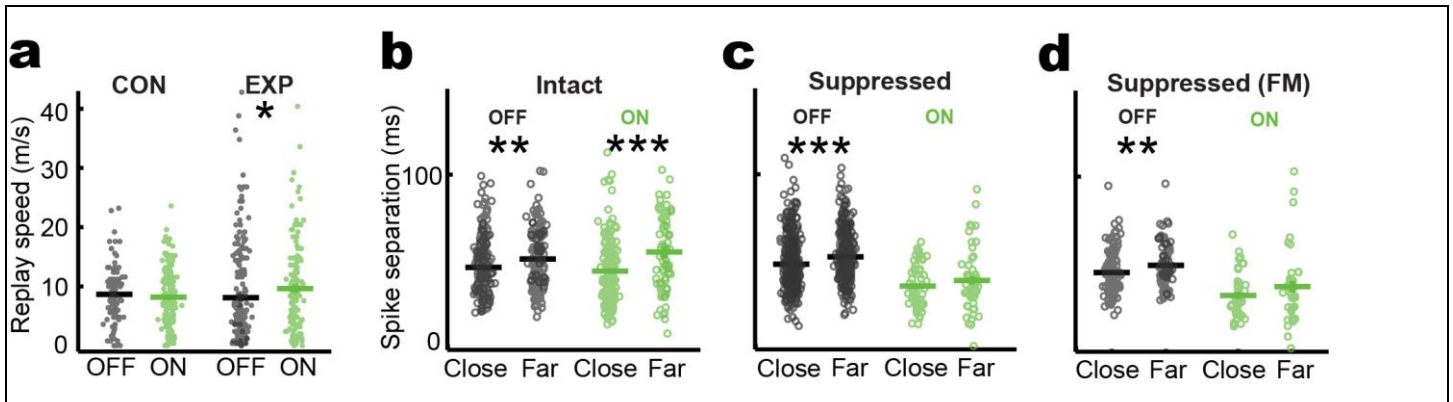
Histogram of theta phase precession characteristics, including precession onset (a), range (b), quality as reflected in the correlation coefficient (c), and slope (d). Distribution of each characteristic in light OFF (black) and light ON (green) conditions is shown in CON (left) and EXP (right) rats. The fraction of place fields with significant phase precession ($p < 0.05$) are shown with filled color. For each place field, the number of spikes during each light condition was considered as the number of samples (“n”) for that light condition and the significance (p-value) of theta precession for that place field was defined using a circular-linear regression method described in section “Theta phase locking and phase precession” in Online Methods. The statistics of the histograms in a, b, c, and d are respectively shown in Figure 3d, Supplementary Figure 8f, Figure 3e, and Supplementary Figure 8g.



Supplementary Figure 10

Lap-by-lap Bayesian decoding of behavior of an EXP rat

Bayesian decoding of population posterior probability (heat plot) of rat's position as it traverses the linear track is overlaid with its factual position (cyan dashed line) in light OFF and light ON (depicted by green bar) conditions. Only the returning direction in each lap is shown.



Supplementary Figure 11

Awake replays and pairwise reactivations are degraded in EXP rats during light ON condition.

a Replay speed is higher in EXP replays during light ON condition (CON: OFF: 8.66 ± 0.48 (mean \pm s.e.m for all values in this figure legend) m/s and ON: 8.18 ± 0.41 , two-tailed t-test, $n_1 = 99$ and $n_2 = 148$ replays, $p = 0.45$; EXP: OFF: 8.09 ± 0.57 and ON: 9.62 ± 0.72 , two-tailed rank-sum test, $n_1 = 212$ and $n_2 = 121$ replays, $p = 0.023$).

b In-SWR spike separation for intact place field pairs with close (<65 cm) peaks is shorter than intact pairs with far (>65 cm) peaks in both light OFF and light ON conditions (OFF: Close: 46.03 ± 0.92 ms and Far: 50 ± 1.38 , two-tailed rank-sum test, $n_1 = 269$ and $n_2 = 156$ field pairs, $p = 0.005$; ON: Close: 43.90 ± 1.56 and Far: 55.00 ± 3.3 , two-tailed rank-sum test, $n_1 = 166$ and $n_2 = 75$ field pairs, $p = 0.0008$).

c Spike separation in suppressed field pairs is not preserved during light ON condition (OFF: Close: 47.64 ± 0.54 ms and Far: 51.96 ± 0.65 , two-tailed rank-sum test, $n_1 = 639$ and $n_2 = 444$ field pairs, $p = 10^{-7}$; ON: Close: 34.84 ± 1.58 and Far: 38.17 ± 2.55 , two-tailed rank-sum test, $n_1 = 60$ and $n_2 = 52$ field pairs, $p = 0.45$).

d Spike separation in firing-matched (FM) suppressed field pairs is not preserved during light ON condition (OFF: Close: 44.13 ± 1.04 ms and Far: 48.31 ± 1.14 , two-tailed rank-sum test, $n_1 = 136$ and $n_2 = 98$ field pairs, $p = 0.0017$; ON: Close: 30.79 ± 2.04 and Far: 35.91 ± 3.32 , two-tailed rank-sum test, $n_1 = 41$ and $n_2 = 41$ field pairs, $p = 0.3$). * $P < 0.05$, ** $P < 0.01$, *** $P < 0.001$.